PAPER

Check for updates

Dual-gate low-voltage transparent electric-double-layer thin-film transistors with a top gate for threshold voltage modulation

Wei Dou [ID] *[a] and Yuanyuan Tan[b]

Dual gate (DG) low-voltage transparent electric-double-layer (EDL) thin-film transistors (TFTs) with microporous-SiO_2 for both top and bottom dielectrics have been fabricated, both dielectrics were deposited by plasma-enhanced chemical vapor deposition (PECVD) at room temperature. The threshold voltage of such devices can be modulated from -0.13 to 0.5 V by the top gate (TG), which switches the device from depletion-mode to enhancement-mode. High performance with a current on/off ratio ($\sim 2.1 \times 10^6$), subthreshold swing (76 mV per decade), operating voltage (1.0 V), and field-effect mobility (~ 2.6 cm^2 V^{-1} s^{-1}) are obtained. Such DG TFTs are promising for ion-sensitive field-effect transistors sensor applications with low-power consumptions.

Introduction

In recent years, dual-gate (DG) thin-film transistors (TFTs) with both a top-gate (TG) and a bottom-gate (BG) in the same device structure have been studied by more and more scientists,[1-5] as the configuration offers increased control of tuning the threshold voltage (V_{th}) of TFTs. Proper V_{th} can ensure low power consumption and appropriate operation-mode,[6,7] so DG TFTs are promising for biological/chemical sensor applications and fabrication of complicate circuits.[8,9] Tuning threshold voltage by varying thickness has been reported by Lee et al.,[10] however, the TFTs with a thick body operating in depletion-mode suffer from enlargement of the subthreshold swing and the leakage current.

In this letter, DG a-IGZO electric-double-layer (EDL) TFTs that can adjust the threshold voltage in both positive and negative directions with a TG have been fabricated on glass substrates at room temperature. By changing the voltage biases of BG, the threshold voltage can be significantly moved from -0.13 to 0.5 V, so such DG TFTs can operate in both depletion-mode and enhancement-mode. Besides, as compared with the standard single gate devices (STD devices), this DG TFT with a TG shows a lower leakage current and an almost unchanged subthreshold swing. Such transparent devices also exhibit a field-effect mobility of ~ 2.6 cm^2 V^{-1} s^{-1}, high on/off ratio of $\sim 2.13 \times 10^6$, low subthreshold swing of 76 mV per decade at a low operating voltage of 1.0 V. These results demonstrate potential applications in low power and high performance

transparent electronics. The switching stability of such DG TFTs with a top gate is also discussed.

Experimental

The entire process of device fabrication was performed at room temperature. First, a 2 μm-thick SiO_2 electrolyte film was deposited by plasma-enhanced chemical vapor deposition (PECVD) on transparent conducting ITO glass substrates using SiH_4 and O_2 mixture as reactive gases. Second, a 40 nm-thick IGZO active channel was deposited by RF magnetron sputtering using a power of 100 W and a working pressure of 0.5 Pa in argon. Third, 2 μm-thick SiO_2 electrolyte film was deposited by plasma-enhanced chemical vapor deposition (PECVD) using a SiH_4 and O_2 mixture as reactive gases as top dielectric layer. At last, the fabrication of the TFT arrays was completed by RF sputtering of 200 nm-thick highly conducting ITO source/drain and top-gate electrodes through a nickel shadow mask. The channel length and width are 80 and 1000 μm, respectively. For comparison, the standard single gate devices were also fabricated under the same condition. Optical analysis is performed by ultraviolet spectrophotometer (Lambda 950). Electrical characterizations of both STD and DG TFTs were performed by a semiconductor parameter analyzer (Keithley 4200 SCS).

Results and discussion

Fig. 1a shows the schematic diagram of the fabricated dual-gate low-voltage transparent EDL TFT with the driving bottom gate and the control top-gate. The optical transmission spectra of as-fabricated TFT arrays on glass substrates (the thickness of the glass substrate is 1.5 mm) is shown in Fig. 1b, the TFT arrays on glass substrates show an optical transmittance of over 80%. The

[a]Key Laboratory of Low Dimensional Quantum Structures and Quantum Control, College of Physics and Electronics Science, Hunan Normal University, Changsha, 410081, People's Republic of China. E-mail: douwei139@163.com

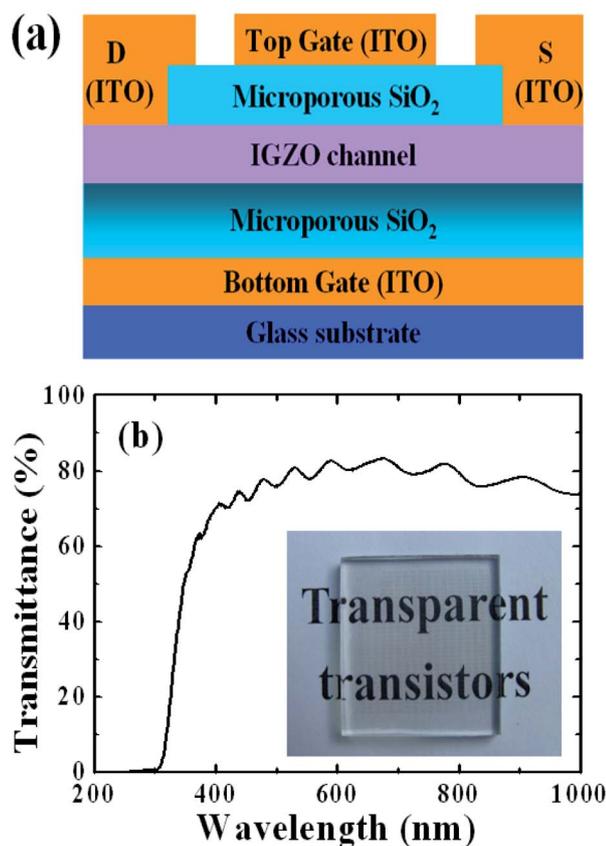[b]Hunan First Normal University, Changsha, 410205, People's Republic of China

Fig. 1 (a) Structure of the dual-gate TFT with the driving bottom gate and the control top-gate. (b) Optical transmission spectra of such TFT arrays on glass substrates. Inset: an optical image of the TFT arrays placed on background text.
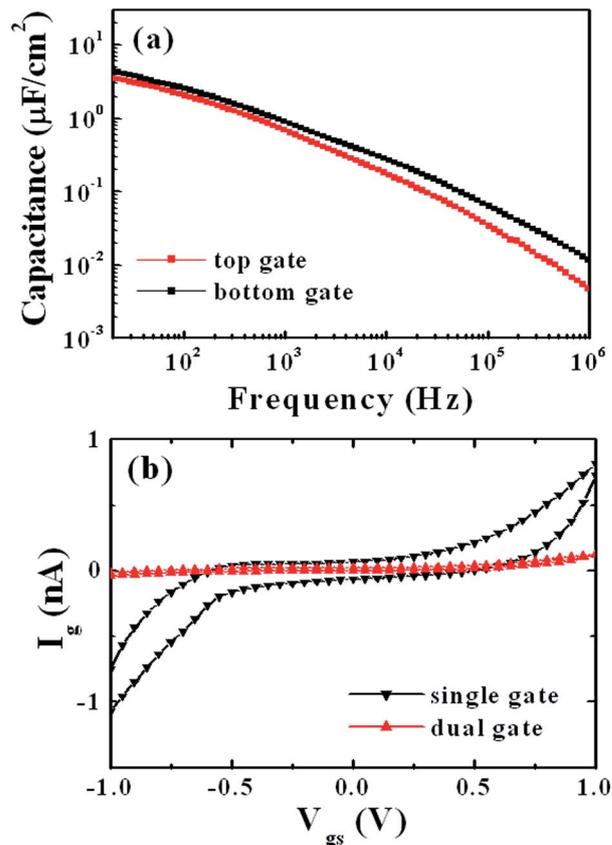

Fig. 2 (a) Specific gate capacitance of the TG and BG dielectrics of such DG TFTs. (b) Leakage current of the STD and DG TFTs.

inset in Fig. 1b shows a photograph of a transparent TFT array chip placed over some background text. We can see the letter through the TFT chip, indicating the TFT arrays are fully transparent to visible light.

As shown in Fig. 2a, like other microporous-SiO$_2$ in the previous work reported by our groups,[11] these TG and BG dielectrics of such DG TFTs also show huge specific capacitance of ~4 µF cm^{-2} at 20 Hz, which leads to a low operating voltage of 1.0 V. Fig. 2b shows the leakage current of the STD and DG TFTs. The leakage current of STD TFTs was ~1 nA, however, the leakage current of DG TFTs was less than 0.2 nA, which was much smaller than that of solid polymer electrolytes or ionic liquids.[12,13] Despite the nanopores existed in double gate dielectrics, the leakage current is five orders of magnitude smaller than the channel current, which guarantees the device performance will not be affected by the leakage current.

The initial electric characteristics of such device are estimated as the conventional BG TFTs. The electron field-effect mobility (μ_{sat}) in the saturation regime is calculated using the relationship $I_{ds} = (WC_{bg}/2L)\mu_{sat}(V_{bg} - V_{th})^2$, where $L = 80$ µm and $W = 1000$ µm are the channel length and width, respectively. The field-effect mobility is calculated to be ~2.6 cm^2 V^{-1} s^{-1} at $V_{ds} = 1.0$ V, $V_{bg} = 1.0$ V. The corresponding carrier density

of the IGZO channel layer is estimated to be 3.5×10^{13} cm^{-2} by $N = C_{bg}(V_c - V_{on})/e$. $C_{bg} = 4.0$ µF cm^{-2} is the bottom gate specific capacitance at 20 Hz. The $V_c = 1.0$ V is the bottom gate voltage bias for mobility estimation. $V_{on} = -0.4$ V is the turn-on voltage of the device without a top gate bias. Fig. 3a shows the transfer characteristics of the DG TFTs in the saturation regime ($V_{ds} = 1.0$ V) with top gate voltage biases in the range from 2.0 V to −2.0 V. All transfer curves were sweeping from negative to positive with a negative bias stress time of 10 s and a sweep rate of 50 mV s^{-1}. The hysteresis window is less than 0.05 V upon sweeping forward and backward without obvious bias stress effect. Thus, we only plotted the result of forward sweeps. When V_{tg} is swept from 2.0 V to −2.0 V, the transfer curves systematically shift from left to right. Fig. 3b shows the $(I_{ds})^{1/2}$–V_{bg} transfer curves with different V_{tg}. The threshold voltage (V_{th}), indicated by the intercepts lines with the V_{bg} axis, moves from a negative value of −0.13 V to a positive value of 0.5 V. These results indicate that an effectively electrostatic coupling is realized between the top gate and the IGZO channel. By the way, subthreshold swing of ~76 mV per decade and current on/off ratio of ~2.1 × 10^6 are almost constant at various voltage biases of top gate.

Fig. 4a and b show the output characteristics of transparent dual-gate TFTs with different voltage bias of top gate. Linear behaviours of I_{ds} at low V_{ds} are observed, indicating that good
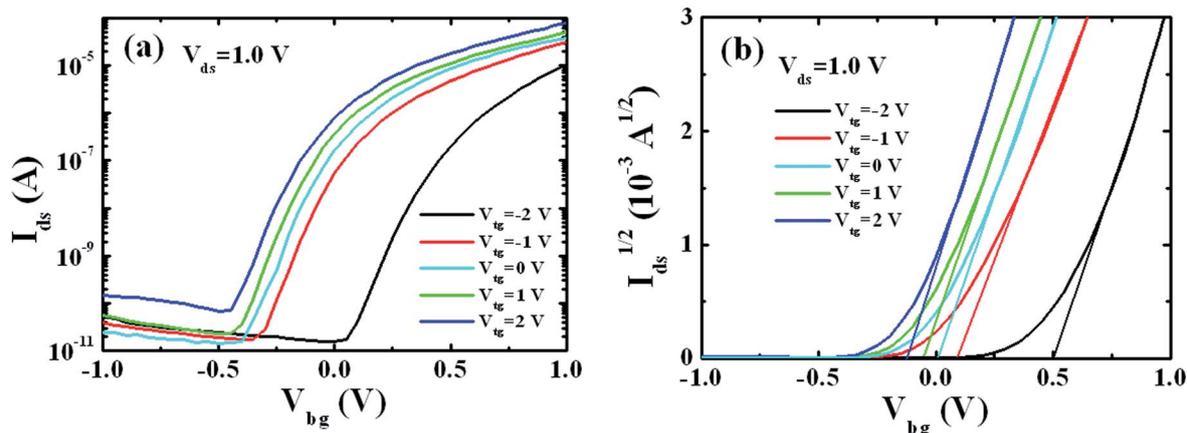
Fig. 3 (a) The transfer characteristics of the dual-gate TFTs at different top-gate voltage biases. (b) $(I_{ds})^{1/2}-V_{bg}$ curves of the same device.
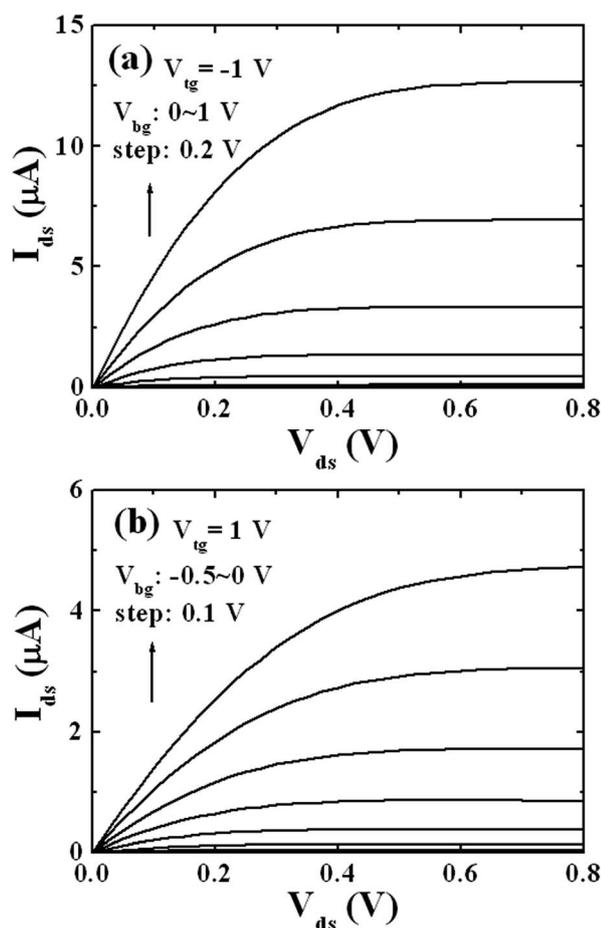

Fig. 4 Output characteristic of the dual-gate TFTs operated at enhancement mode (a) when $V_{tg} = -1.0$ V, at depletion mode (b) when $V_{tg} = 1.0$ V.

ohmic contact between the IGZO channel layer and ITO source/drain electrodes were realized. When V_{tg} was changed from 2.0 V to −2.0 V, depletion-mode was gradually changed to enhancement-mode. So dual-gate configuration provides more flexibility in device operation.

The extracted V_{th} and subthreshold swing (S) are presented in Fig. 5a as a function of the V_{tg} for DG TFTs. The asymmetric behaviour of V_{th} shift is due to the changeable $C_{bg-dielectric}$ and $C_{tg-dielectric}$ at different (positive and negative) V_{tg}. When $V_{tg} \geq$ 0 V, all ITO electrodes are highly conducting, and the capacitance values of $C_{bg-dielectric}$ (C_{bd}) and $C_{tg-dielectric}$ (C_{td}) are
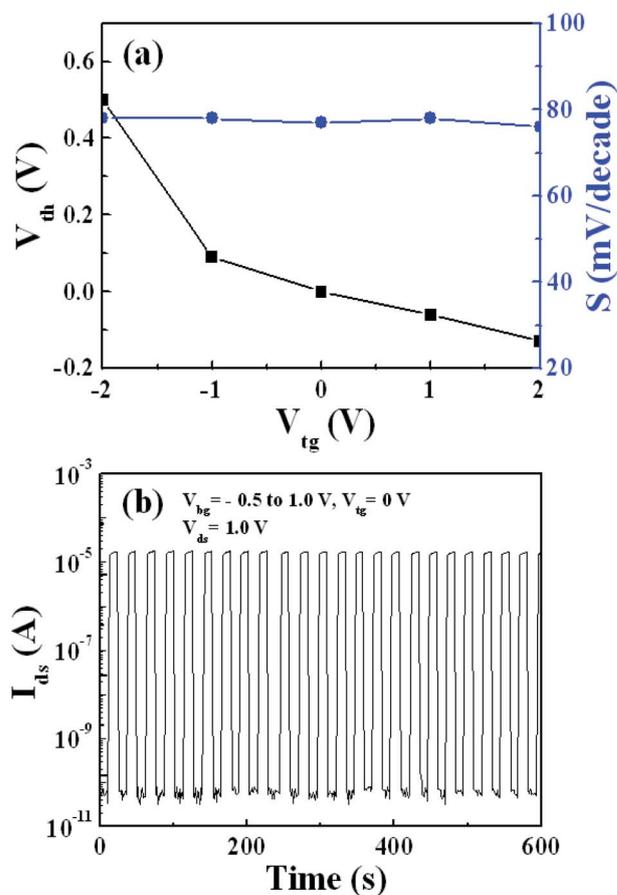

Fig. 5 (a) The threshold voltage and subthreshold swing of the dual gate TFTs at different V_{tg}. (b) The switching stability driven by square-wave pulses with a period of 1 Hz.

equivalent to the EDL capacitance of SiO_2-based electrolyte. When $V_{tg} < 0$ V, C_{bd} and C_{td} will become smaller due to the IGZO film depletion effect induced by the negative V_{tg}. According to the equation: $\Delta V_{th} = \Delta V_{tg} C_{td}/[C_{td} + (C_{bd} + C_{td})]$, a larger V_{th} shift can be obtained when $V_{tg} < 0$ V. These results indicates that the V_{th} is very sensitive to the changes in the surface potential of the top gate dielectric region,[14] so such DG TFTs are very promising for ion-sensitive field-effect transistors sensor applications. Simultaneously, the S has a weak dependence on the top gate bias, which indicates the value of S was almost unaffected by the V_{tg}. Such DG TFTs were continuously switched between the ON- and OFF-states in dynamic stress tests (periodic square-wave pulses of $V_{bg} = -0.5$ to -1.0 V, $V_{tg} = 0$ V, and $V_{ds} = 1.0$ V), as shown in Fig. 5b. A drain-current on/off ratio of larger than 10^5 was maintained, and no obvious drain current decrease was observed. This result suggests very good switching stability of the DG TFTs with a top gate.

Conclusions

In conclusion, dual-gate low-voltage transparent EDL TFTs gated by PECVD-deposited microporous-SiO_2 were fabricated with a top gate. Carrier density of the channel, V_{th} and operation mode of the devices can be tuned by the top gate. The V_{th} of such device can be systematically tuned from -0.13 V to 0.5 V by using a top-gate bias ranging from 2.0 V to -2.0 V. The combination of the controllability of V_{th}, room temperature process, low-voltage operation of the transparent dual-gate TFTs are very promising for ion-sensitive field-effect transistors sensor applications.

Author contributions

Thin-film transistor and device performance was fabricated and characterized by W. D. The manuscript was prepared by W. D. and Y. T. W. D. examined and commented on the manuscript. The project was guided by W. D.

Conflicts of interest

There are no conflicts to declare.

Acknowledgements

Notes and references

1 M. Chun, J. G. Um, M. S. Park, M. D. H. Choudhury and J. Jang, *AIP Adv.*, 2016, **6**, 075217.

2 J. C. Dutta, H. R. Thakur and G. Keshiwani, *IEEE Sens. J.*, 2019, **19**, 5692–5699.

3 Y. Kamada, S. Fujita, M. Kimura, T. Hiramatsu, T. Matsuda, M. Furuta and T. Hirao, *IEEE Electron Device Lett.*, 2011, **32**, 509.

4 J. Jiang, J. Sun, L. Zhu, G. Wu and Q. Wan, *Appl. Phys. Lett.*, 2011, **99**, 113504.

5 J. Sun, J. Jiang, W. Dou and Q. Wan, *IEEE Electron Device Lett.*, 2011, **32**, 1710.

6 W. Dou and Y. Tan, *ACS Omega*, 2019, **4**, 21417.

7 W. Dou, L. Zhu, J. Jiang and Q. Wan, *Appl. Phys. Lett.*, 2013, **102**, 093509.

8 D. Kasprowicz, *IEEE Trans. Comput. Aided Des. Integrated Circ. Syst.*, 2019, **7**, 10389–10393.

9 K. Tamersit, *J. Comput. Electron.*, 2019, **18**, 846–855.

10 J. M. Lee, I. T. Cho, J. H. Lee and H. I. Kwon, *Jpn. J. Appl. Phys.*, 2009, **48**, 100202.

11 W. Dou and Y. Tan, *RSC Adv.*, 2019, **9**, 30715.

12 J. H. Cho, J. Lee, Y. Xia, B. Kim, Y. Y. He, M. J. Renn, T. P. Lodge and C. D. Frisbie, *Nat. Mater.*, 2008, **7**, 900.

13 L. Zhao, K. Chen, F. Yang, M. L. Zheng, J. M. Guo, G. Q. Gu, B. Zhang, H. F. Qin, G. Cheng and Z. L. Du, *Nano Energy*, 2019, **62**, 38–45.

14 M. J. Spijkman, J. J. Brondijk, T. T. Geuns, E. P. Smits, T. Cramer, F. Zerbetto, P. Stoliar, F. Biscarini, P. M. Blom and D. M. Leeuw, *Adv. Funct. Mater.*, 2010, **20**, 898.